Geochemical Journal, Vol. 43, pp. 235 to 246, 2009

Mn/Ca ratio in planktonic foraminifer from ODP Site 1144, the northern South China Sea: A possible paleoclimate indicator

GANG-JIAN WEI,[1]* LIANG ZOU,[1,3] WEN-FENG DENG,[1] XIAN-HUA LI,[1] YING LIU[1] and JIAN-FANG CHEN[2]

[1]Key Laboratory of Isotope Geochronology and Geochemistry, Guangzhou Institute of Geochemistry, Chinese Academy of Sciences, Guangzhou 510640, China
[2]The Second Institute of Oceanography, SOA, Hangzhou 310012, China
[3]Graduate School of the Chinese Academy of Sciences, Beijing 100039, China

(*Received April 18, 2008; Accepted January 15, 2009*)

We report here high-resolution Mn/Ca ratios of planktonic foraminifer, *Globigerinoides sacculifer* from ODP Site 1144 in the northern South China Sea (SCS). The variation pattern of the Mn/Ca ratios of *G. sacculifer* from the top 170 mcd is very similar to those of the generally used paleoclimate records, such as $\delta^{18}O$ of *Globigerinoides ruber* and SSTs derived from Mg/Ca ratios of *G. sacculifer*. Robust Milankovitch periodicities are presented in the power spectrum of the Mn/Ca record, as well as in those of the other paleoclimate records, suggesting orbital forcing for the variation of the Mn/Ca ratios. Further spectral analysis indicates that the variations of the Mn/Ca ratios lead those of the $\delta^{18}O$ of *G. ruber* at all the orbital periodicities, and are roughly in pace with or slightly lead those of the SSTs at eccentricity and obliquity periodicities, but lag behind that of the SSTs at precession periodicity. This suggests that the driven forcing for the variation of the Mn/Ca ratios mainly associate with those for the SSTs. Comparisons between the Mn/Ca ratios and other geochemical proxies for redox condition in sediments show that higher Mn/Ca ratios of *G. sacculifer* generally correspond to higher authigenic Mn concentrations and lower contents of total sulfur (TS) and total organic carbon (TOC). Thus, the Mn coatings in the *G. sacculifer* at ODP Site 1144 are mainly associated with Mn oxides, and the variation of the Mn/Ca ratios of *G. sacculifer* appears to indicate changes of redox condition in sediments. Exception is observed at the top 10 mcd, in which the Mn/Ca ratios show an upward decreasing trend and low core-top values, while other proxies suggest oxic environment in this section. The low Mn/Ca ratios agree with the general low Mn/Ca ratios in foraminifer tests from core-top sediments in the SCS, and seem to attribute to the fact that authigenic Mn precipitation are mainly generated within sediment column rather than at sediment surface and the oxidation states for them may change from Mn(III) oxyhydroxides to Mn(IV) oxides after burial. However, details are not well known yet. Despite of such uncertainties, the response of the variation of the Mn/Ca ratios of *G. sacculifer* to paleoclimate changes is significant, indicating that it is an informative paleoclimate indicator.

Keywords: planktonic foraminifer, Mn/Ca ratios, paleoclimate proxy, South China Sea, ODP

INTRODUCTION

Mn coatings have generally been observed to overgrow on foraminifer tests from marine sediments around the world. There are at least two types of Mn coatings on foraminifer tests, one may be Mn oxides, and the other seems to be a mixed calcium–manganese–magnesium carbonate (Boyle, 1983; Pena *et al*., 2005). These materials tend to concentrate some minor and trace elements, and are considered as potential contaminants when measuring trace elements in foraminifera tests (Boyle, 1981). Studies in the past decade indicate that Mg/Ca ratio in planktonic foraminifer tests is a good proxy for sea surface temperature (SST) (Hastings *et al*., 1998; Lea *et al*., 1999; Nürnberg *et al*., 1996; Rosenthal *et al*., 2000), and has been broadly used in reconstructing SST records (Elderfield and Ganssen, 2000; Lea *et al*., 2002, 2006; Mashiotta *et al*., 1999; Nürnberg and Groeneveld, 2006). Accompanying with these studies, debates on whether Fe–Mn coatings significantly contaminate Mg/Ca ratios in foraminifera tests or not have never stopped. Some studies indicate that Mg/Ca ratios in foraminifera tests decrease significantly after removing the Fe–Mn coatings by a reductive cleaning step, in which a buffered solution of hydrous hydrazine is used (Pena *et al*., 2005; Weldeab *et al*., 2006). Other studies, however, indicate that removal of Fe–Mn coatings seems not significantly influence Mg/Ca ratios in foraminifera tests (Hastings *et al*., 1998), and the observed significant Mg/Ca decrease may be the result of partial dissolution of foraminifera tests during

*Corresponding author (e-mail: gjwei@gig.ac.cn)

reductive cleaning procedure (Barker *et al.*, 2003; Yu *et al.*, 2007). Whether it is necessary to adopt a reductive cleaning procedure to remove Fe–Mn coatings in Mg/Ca ratio measurements depends on Mn concentrations in foraminifera tests (Wei *et al.*, 2007). Such conflicts are mainly attributed to the different behaviors of these two types of Mn coatings. Ca–Mg–Mn carbonates are likely formed in extreme reductive environments (Boyle, 1983), whereas Mn oxides are generally deposited from oxic water column (Landing and Bruland, 1987), and act as important oxidants during early diagenesis in marine sediments (Froelich *et al.*, 1979). Serious Mg contaminations are mainly contributed from Ca–Mg–Mn carbonates, and the contribution from Mn oxides is generally negligible (Pena *et al.*, 2005). Thus, the redox condition in sediments may determine which phase dominates the Mn coatings in foraminifer tests, and hence control the extent of Mg contaminations.

No matter what they are considered, serious contaminants to be removed or negligible materials without much contamination, details of the Mn coatings in foraminifer tests are still not well-known currently. For instance, when they overgrow on foraminifer tests, in water column or after buried, how they vary during early diagenesis, and what kind of factors control their variations. Lack of such knowledge obscures our understanding of the nature of the Mn coatings, and hinders the evaluation of their influences in geochemical analysis on foraminifer tests. Changes of Mn concentrations in foraminifer tests may help to answer these questions. Deposited as Mn oxides in oxic environments, and consequently dissolved during diagenesis (Froelich *et al.*, 1979; Landing and Bruland, 1987), Mn is very sensitive to changes of redox conditions in sediments. Changes of authigenic Mn concentrations in sediments have generally been considered to indicate redox conditions (Froelich *et al.*, 1979; Mangini *et al.*, 1990, 2001). However, the variations of Mn concentrations in foraminifer tests are less concerned in the previous studies even though they are potentially informative to climatic/environmental changes.

Herein, we report the high-resolution Mn/Ca ratios of planktonic foraminifer, *G. sacculifer*, from the top 170 mcd (meters composite depth) sediments at ODP Site 1144, the northern South China Sea (SCS). These Mn/Ca ratios were simultaneously measured with Mg/Ca ratios for the aim of estimating Mg contaminations from Mn coatings (Wei *et al.*, 2007). It will be shown that the Mn/Ca ratios reveal an obvious climatic-controlled variation pattern. Comparison between the Mn/Ca ratios and other paleoclimate records will be made, and the possible driven forcing for the change of the Mn/Ca ratios will be discussed. The aim of this work is to find more insight about the variations of Mn concentrations in foraminifer tests. This is helpful for a better understanding of the origin of the Mn coatings, and benefits seeking for more information of climatic and environmental changes from planktonic foraminifer.

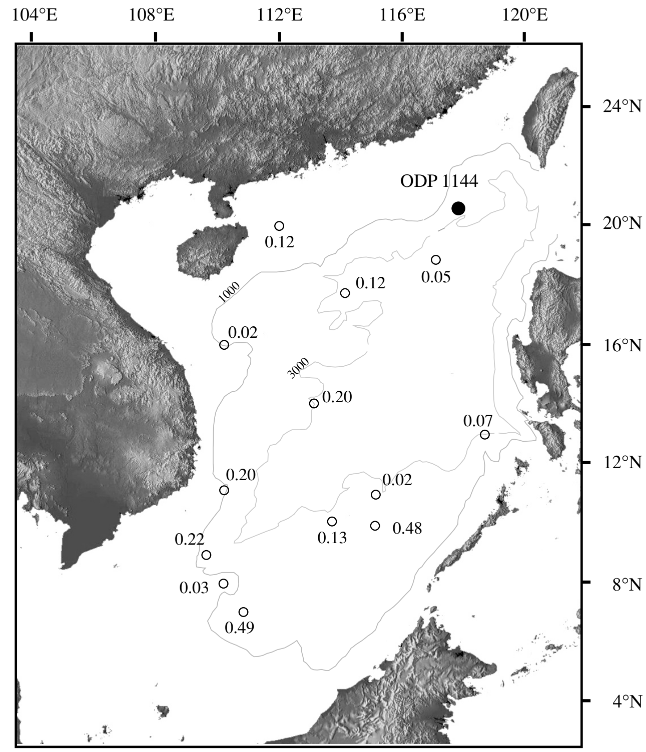

Fig. 1. The location of ODP Site 1144 in the South China Sea. The image indicates the land and islands, and the thin lines indicate the isobaths of 1000 m and 3000 m. The filled circles indicate the locations of ODP Site 1144. The open circles indicate the locations of core-top sediments discussed in the text, and the data next to them are the Mn/Ca ratios (unit: mmol/mol) of G. sacculifer from these core-top sediments.

MATERIALS AND METHODS

The sediment cores were drilled at ODP Site 1144 (20°3.18′ N, 117°25.14′ E, at water depth of 2037 m) during Leg 184 cruise (Fig. 1). Sedimentary rates of the top 220 mcd of these cores are very high, up to 84.8 cm/kyr (Shipboard Scientific Party, 2000). The studied sediment samples were gathered in the hole A from the top to core 17H in an average interval of about 50 cm, corresponding to a time resolution of about 0.2~0.5 kyr.

The >250 μm *G. sacculifer* tests were hand picked from the wet sieved components for measurement. The tests were first crushed into pieces to open the chamber before cleaning. Three cleaning steps were performed on these samples, including ultrasonically washing in deionized water and distilled alcohol, respectively, to remove adhered clay minerals, and washing in a hot alka-

Table 1. Mn/Ca ratios of G. sacculifer from the sediments at ODP Site 1144

mcd	Age* (kyr)	Mn/Ca (mmol/mol)	mcd	Age* (kyr)	Mn/Ca (mmol/mol)	mcd	Age* (kyr)	Mn/Ca (mmol/mol)
1.00	1.78	0.361	18.91	19.32	0.141	34.66	30.16	0.143
1.37	2.42	0.267	19.45	19.62	0.139	34.77	30.25	0.265
1.87	3.29	0.332	19.56	19.68	0.170	35.28	30.65	0.228
2.02	3.55	0.290	20.01	19.93	0.197	35.66	30.96	0.244
2.49	4.36	0.327	20.44	20.17	0.146	36.16	31.35	0.159
2.87	5.02	0.223	20.95	20.46	0.179	36.91	32.02	0.297
3.37	5.89	0.340	21.05	20.51	0.142	37.40	32.52	0.342
3.52	6.15	0.259	21.49	20.76	0.190	37.80	32.94	0.197
4.42	7.72	0.285	21.91	20.99	0.204	38.30	33.45	0.344
4.87	8.50	0.381	22.35	21.24	0.223	38.41	33.56	0.273
5.02	8.76	0.327	22.49	21.31	0.186	38.91	34.05	0.273
5.87	10.24	0.409	23.00	21.60	0.137	39.30	34.40	0.315
6.37	11.10	0.501	23.43	21.84	0.179	39.87	34.93	0.311
6.48	11.30	0.437	23.88	22.09	0.222	39.97	35.02	0.312
6.97	11.92	0.369	23.99	22.15	0.153	40.52	35.52	0.195
8.75	13.36	0.660	24.49	22.42	0.183	40.83	35.81	0.257
9.22	13.74	0.547	24.88	22.64	0.143	41.31	36.25	0.282
9.62	14.06	0.738	25.38	22.92	0.264	42.02	36.85	0.287
10.12	14.44	0.733	25.49	22.98	0.181	42.33	37.08	0.404
10.22	14.49	0.587	25.99	23.26	0.182	42.87	37.48	0.482
10.77	14.80	0.609	26.38	23.49	0.266	42.96	37.54	0.641
11.13	14.99	0.607	26.88	23.80	0.239	43.52	37.95	0.356
11.67	15.30	0.332	27.27	24.12	0.212	43.83	38.18	0.301
11.77	15.35	0.315	27.77	24.53	0.195	44.30	38.57	0.251
12.27	15.63	0.302	28.16	24.85	0.232	44.41	38.67	0.298
12.73	15.89	0.304	28.66	25.27	0.172	44.91	39.12	0.206
13.09	16.09	0.294	28.77	25.36	0.202	45.30	39.46	0.234
13.27	16.19	0.196	29.36	25.84	0.153	45.80	39.91	0.247
13.87	16.52	0.217	29.69	26.11	0.244	48.35	42.19	0.266
14.13	16.67	0.166	30.17	26.51	0.235	48.85	42.61	0.303
14.67	16.97	0.152	30.33	26.64	0.237	49.26	42.86	0.348
14.77	17.02	0.201	30.86	27.07	0.163	49.74	43.16	0.423
15.22	17.27	0.152	31.18	27.34	0.155	49.85	43.23	0.388
15.67	17.52	0.160	31.67	27.74	0.183	50.36	43.55	0.293
16.12	17.77	0.120	31.83	27.87	0.185	50.74	43.79	0.347
16.27	17.86	0.121	32.38	28.32	0.147	51.24	44.10	0.363
16.73	18.11	0.122	32.66	28.55	0.208	51.37	44.18	0.283
17.16	18.35	0.232	33.16	28.96	0.143	52.18	44.69	0.350
17.66	18.63	0.076	33.27	29.05	0.188	52.25	44.73	0.382
17.99	18.81	0.157	33.76	29.44	0.176	52.71	45.02	0.283
52.91	45.15	0.301	63.58	55.23	0.394	73.57	64.74	0.349
52.92	45.15	0.344	63.63	55.28	0.365	73.65	64.81	0.285
53.37	45.51	0.368	63.95	55.58	0.444	73.68	64.83	0.394
53.46	45.58	0.416	64.23	55.85	0.439	74.14	65.24	0.416
53.76	45.85	0.326	64.25	55.87	0.477	74.17	65.27	0.292
53.80	45.89	0.341	64.74	56.34	0.390	74.54	65.59	0.296
54.25	46.32	0.265	64.78	56.38	0.334	74.57	65.62	0.268
54.30	46.37	0.280	65.10	56.73	0.603	75.04	66.04	0.374
54.37	46.43	0.324	65.13	56.76	0.460	75.04	66.04	0.349
54.40	46.46	0.288	65.59	57.27	0.426	75.15	66.13	0.302
54.90	46.94	0.371	65.63	57.31	0.350	75.20	66.18	0.244
54.96	46.99	0.445	65.73	57.42	0.430	75.64	66.57	0.380
55.27	47.29	0.533	65.75	57.44	0.392	75.66	66.58	0.316
55.30	47.32	0.364	66.25	57.99	0.420	76.04	66.92	0.332
55.71	47.71	0.465	66.28	58.02	0.373	76.07	66.95	0.327
55.74	47.74	0.363	66.60	58.35	0.333	76.54	67.36	0.507
55.90	47.89	0.387	66.63	58.38	0.305	76.59	67.41	0.393
55.92	47.91	0.448	67.05	58.77	0.295	76.65	67.46	0.310
56.41	48.38	0.475	67.07	58.80	0.293	76.69	67.50	0.325

Table 1. (continued)

mcd	Age* (kyr)	Mn/Ca (mmol/mol)	mcd	Age* (kyr)	Mn/Ca (mmol/mol)	mcd	Age* (kyr)	Mn/Ca (mmol/mol)
56.45	48.42	0.550	67.23	58.95	0.304	77.14	67.89	0.347
56.76	48.71	0.525	67.23	58.95	0.357	77.16	67.91	0.332
56.80	48.75	0.376	67.74	59.43	0.297	77.54	68.25	0.347
57.25	49.18	0.444	67.78	59.47	0.247	77.59	68.29	0.426
57.30	49.23	0.481	68.08	59.75	0.367	78.01	68.69	0.307
59.68	51.51	0.475	68.14	59.80	0.322	78.04	68.73	0.308
59.71	51.53	0.387	68.57	60.21	0.274	78.15	68.87	0.351
60.17	51.97	0.494	68.60	60.24	0.190	78.19	68.92	0.438
60.20	52.00	0.576	70.65	62.15	0.203	78.67	69.55	0.384
60.57	52.36	0.383	70.70	62.20	0.279	79.04	70.04	0.473
60.59	52.38	0.464	71.15	62.59	0.325	79.09	70.10	0.500
61.10	52.86	0.507	71.17	62.61	0.250	79.54	70.69	0.502
61.18	52.94	0.339	71.54	62.94	0.349	79.59	70.76	0.543
61.21	52.96	0.322	71.58	62.98	0.381	79.82	71.06	0.463
61.67	53.41	0.381	72.04	63.38	0.372	79.85	71.10	0.437
61.70	53.43	0.348	72.07	63.41	0.405	80.30	71.69	0.424
62.08	53.80	0.360	72.15	63.48	0.366	80.32	71.71	0.173
62.13	53.85	0.448	72.17	63.50	0.328	80.70	72.21	0.533
62.45	54.15	0.560	72.65	63.92	0.280	80.75	72.28	0.576
62.72	54.41	0.379	72.67	63.94	0.202	81.20	72.87	0.545
62.73	54.42	0.427	73.04	64.27	0.204	81.25	72.94	0.494
63.23	54.90	0.257	73.07	64.29	0.245	81.33	73.06	0.515
63.28	54.95	0.319	73.54	64.71	0.272	81.38	73.13	0.519
81.78	73.72	0.536	91.70	86.47	0.212	100.08	95.35	0.554
81.92	73.92	0.426	92.09	86.81	0.325	100.13	95.41	0.577
82.17	74.30	0.535	92.13	86.85	0.360	100.76	96.17	0.582
82.25	74.42	0.205	92.58	87.24	0.453	100.80	96.22	0.581
82.72	75.11	0.360	92.63	87.28	0.397	101.25	96.76	0.583
82.77	75.18	0.637	92.74	87.38	0.404	101.27	96.79	0.551
82.85	75.30	0.598	93.18	87.76	0.380	101.64	97.24	0.664
82.87	75.33	0.630	93.19	87.77	0.336	101.68	97.29	0.490
83.32	76.00	0.544	93.59	88.12	0.518	102.14	97.84	0.576
83.42	76.14	0.574	93.63	88.15	0.505	102.17	97.88	0.573
83.67	76.51	0.455	94.08	88.54	0.446	102.25	97.98	0.445
83.75	76.63	0.363	94.12	88.58	0.523	102.27	98.00	0.487
84.17	77.24	0.487	94.19	88.64	0.634	102.75	98.57	0.580
84.18	77.27	0.332	94.23	88.67	0.440	102.77	98.60	0.645
84.35	77.52	0.285	94.69	89.07	0.414	103.14	99.05	0.673
84.36	77.53	0.450	94.78	89.15	0.408	103.17	99.09	0.651
84.78	78.15	0.460	95.08	89.41	0.494	103.64	99.66	0.535
84.91	78.34	0.493	95.13	89.46	0.524	103.67	99.69	0.450
85.17	78.73	0.503	95.55	89.87	0.490	103.76	99.80	0.678
85.25	78.85	0.339	95.58	89.90	0.585	103.79	99.84	0.595
85.71	79.52	0.508	95.69	90.04	0.487	104.24	100.50	0.524
85.76	79.60	0.410	95.73	90.09	0.507	104.27	100.57	0.520
85.86	79.75	0.370	96.18	90.63	0.504	104.64	101.41	0.616
85.88	79.78	0.583	96.20	90.65	0.451	104.67	101.48	0.636
86.28	80.37	0.404	96.59	91.13	0.542	105.14	102.55	0.404
86.41	80.56	0.388	96.63	91.17	0.504	105.17	102.62	0.477
86.67	80.94	0.426	97.05	91.68	0.585	105.25	102.80	0.427
86.75	81.06	0.315	97.08	91.72	0.585	105.28	102.87	0.429
87.17	81.68	0.390	97.19	91.85	0.603	105.74	103.92	0.465
87.20	81.73	0.292	97.23	91.90	0.574	105.77	103.99	0.466
87.36	81.96	0.356	97.68	92.44	0.538	106.14	104.83	0.631
87.41	82.04	0.157	97.70	92.47	0.517	106.17	104.90	0.653
87.78	82.58	0.310	98.09	92.93	0.647	106.64	105.97	0.695
87.91	82.78	0.335	98.13	92.99	0.501	106.67	106.04	0.659
88.17	83.16	0.288	98.55	93.50	0.502	106.75	106.22	0.753
88.25	83.28	0.334	98.58	93.53	0.582	106.78	106.29	0.724

Table 1. (continued)

mcd	Age* (kyr)	Mn/Ca (mmol/mol)	mcd	Age* (kyr)	Mn/Ca (mmol/mol)	mcd	Age* (kyr)	Mn/Ca (mmol/mol)
88.71	83.87	0.299	98.69	93.67	0.545	107.24	107.83	0.823
88.77	83.92	0.414	98.73	93.72	0.519	107.27	107.93	0.888
91.19	86.03	0.546	99.18	94.26	0.604	107.64	109.19	0.594
91.23	86.06	0.318	99.20	94.28	0.516	107.67	109.29	0.612
91.68	86.46	0.298	99.59	94.76	0.545	108.14	110.89	0.831
81.78	73.72	0.536	99.63	94.80	0.626	108.17	110.99	0.603
108.25	111.27	0.852	124.55	139.53	0.230	141.30	153.46	0.206
108.28	111.37	0.798	125.04	139.94	0.243	142.08	154.10	0.419
108.74	112.94	1.006	125.44	140.28	0.257	142.57	154.50	0.483
108.77	113.04	0.970	125.94	140.71	0.368	142.97	154.83	0.326
109.14	114.30	0.815	126.05	140.80	0.339	143.47	155.24	0.495
109.17	114.40	0.979	126.54	141.22	0.354	143.58	155.33	0.485
109.64	116.00	0.298	126.94	141.55	0.302	144.07	155.73	0.306
109.67	116.11	0.781	127.44	141.98	0.294	144.47	156.06	0.346
113.74	130.03	0.889	127.55	142.07	0.336	144.93	156.44	0.406
113.77	130.06	0.588	128.04	142.49	0.376	145.08	156.56	0.387
114.21	130.46	0.903	128.44	142.83	0.551	145.63	157.02	0.394
114.24	130.49	0.877	128.94	143.25	0.399	145.98	157.30	0.359
114.61	130.82	0.778	129.05	143.34	0.395	146.54	157.76	0.403
114.64	130.85	0.993	129.54	143.76	0.297	146.59	157.80	0.423
115.12	131.29	0.676	129.94	144.10	0.265	147.13	158.25	0.441
115.14	131.31	0.576	130.44	144.52	0.263	147.48	158.53	0.595
115.28	131.43	0.879	130.55	144.62	0.253	147.98	158.95	0.281
115.29	131.44	0.666	131.04	145.02	0.290	148.13	159.07	0.352
115.71	131.82	0.762	131.44	145.35	0.340	148.58	159.44	0.330
115.79	131.90	0.931	131.91	145.74	0.350	148.98	159.77	0.383
116.11	132.19	0.437	132.44	146.17	0.450	149.48	160.18	0.441
116.15	132.22	0.657	132.94	146.58	0.318	149.64	160.31	0.418
116.62	132.64	0.612	133.33	146.90	0.383	151.72	162.02	0.617
116.64	132.67	0.651	133.94	147.40	0.355	152.28	162.48	0.386
116.78	132.79	0.530	134.43	147.81	0.262	152.61	162.75	0.584
117.32	133.28	0.470	134.83	148.14	0.331	153.08	163.15	0.492
117.61	133.55	0.470	135.33	148.55	0.250	153.22	163.27	0.564
118.12	134.01	0.413	135.44	148.64	0.300	153.82	163.77	0.498
118.29	134.16	0.483	135.93	149.04	0.241	154.12	164.03	0.479
118.71	134.55	0.402	136.34	149.38	0.169	154.62	164.46	0.630
119.18	134.97	0.272	136.83	149.78	0.297	154.73	164.55	0.561
119.63	135.36	0.351	136.94	149.87	0.257	155.28	165.02	0.510
119.78	135.48	0.418	137.43	150.27	0.364	155.62	165.32	0.497
120.29	135.92	0.382	137.83	150.60	0.277	156.17	165.79	0.523
120.63	136.20	0.478	138.33	151.01	0.261	156.23	165.84	0.604
121.12	136.62	0.431	138.44	151.10	0.319	156.82	166.35	0.579
121.28	136.76	0.468	138.94	151.51	0.221	157.12	166.60	0.523
121.72	137.13	0.343	139.34	151.84	0.349	157.68	167.08	0.641
123.05	138.26	0.427	139.83	152.25	0.286	157.73	167.13	0.510
123.54	138.67	0.344	139.94	152.34	0.298	158.21	167.54	0.537
123.94	139.01	0.419	140.45	152.75	0.391	158.61	167.88	0.479
124.44	139.43	0.440	140.87	153.10	0.389	159.11	168.31	0.366
159.22	168.40	0.432	163.94	172.44	0.644	167.59	176.14	0.447
159.71	168.82	0.449	164.44	172.87	0.409	168.05	176.68	0.390
160.11	169.16	0.407	164.59	173.00	0.589	168.44	177.13	0.359
160.61	169.59	0.535	165.04	173.38	0.578	168.94	177.72	0.357
161.55	170.40	0.553	165.44	173.73	0.523	169.09	177.90	0.425
162.03	170.81	0.580	165.94	174.21	0.489	169.64	178.54	0.417
162.43	171.15	0.591	166.06	174.35	0.530	169.94	178.89	0.393
162.93	171.58	0.507	166.55	174.92	0.556	170.43	179.47	0.460
163.04	171.67	0.556	166.94	175.38	0.461			
163.53	172.09	0.489	167.44	175.96	0.503			

**The age model is from Büehring et al. (2004).*

Table 2. *Mn/Ca ratios of G. sacculifer from core-top sediments in the SCS*

Sample ID	Locations	Mn/Ca (mmol/mol)	Sample ID	Locations	Mn/Ca (mmol/mol)
84-5	109.7°N, 8.97°E	0.22	S013	110.0°N, 16.0°E	0.02
87-53	110.4°N, 7.01°E	0.49	S021	113.0°N, 14.0°E	0.20
90-97	113.5°N, 10.0°E	0.13	S029	110.0°N, 11.0°E	0.20
157	117.3°N, 18.9°E	0.05	S041	110.0°N, 8.00°E	0.03
321	118.7°N, 12.4°E	0.07	S056	115.0°N, 10.0°E	0.48
S003	112.0°N, 20.0°E	0.12	S057	115.0°N, 11.0°E	0.02
S007	114.0°N, 18.0°E	0.12			

line peroxide solution (10% H_2O_2 in 0.1N NaOH at 80°C) to remove organic matters. No reductive cleaning step was performed. Mn/Ca ratios, together with Mg/Ca ratios, were measured on a Varian Vista Pro inductively coupled plasma atomic emission spectrometry (ICP-AES) in Guangzhou Institute of Geochemistry, Chinese Academy of Sciences. The precision for Mn/Ca ratios was better than 3%. Details of the experiments have been described in Wei *et al*. (2007), and the measured Mn/Ca ratios are presented in Table 1.

The age model for this sediment core is available from Büehring *et al*. (2004), which have been constructed on the oxygen isotopes of *G. ruber* and some AMS ^{14}C dating on *G. ruber* and *G. sacculifer* mixtures.

Mn/Ca ratios of *G. sacculifer* tests from several core-top sediments in the SCS were also measured using the same method. The results are listed in Table 2 and shown in Fig. 1.

RESULTS

The Mn/Ca ratios of *G. sacculifer* from core-top sediments in the SCS change from 0.02 mmol/mol to 0.49 moml/mol, and the two maximum Mn/Ca ratios, 0.48 mmol/mol and 0.49 mmol/mol are observed in the southern SCS (Fig. 1).

The variation of the Mn/Ca ratios of *G. sacculifer* from ODP Site 1144 sediments is shown in Fig. 2. The SST records derived from the simultaneously measured Mg/Ca ratios of *G. sacculifer* (Wei *et al*., 2007), and the oxygen isotopes of *G. ruber* (Büehring *et al*., 2004) are also shown together for comparison. The Mn/Ca ratios change from 0.08 mmol/mol to 1.01 mmol/mol, and show similar variation pattern with those of the SSTs and the $\delta^{18}O$ of *G. ruber*. Higher Mn/Ca ratios generally accompany with higher SSTs and more negative $\delta^{18}O$, except for the top 10 mcd, in which Mn/Ca ratios show an upward decreasing trend, from ~0.7 mmol/mol at ~10 mcd to ~0.2 mmol/mol at ~1 mcd. The variation of Mn/Ca ratios is roughly in pace with the SST and the $\delta^{18}O$ of *G. ruber*. However, some of the main Mn/Ca variations do not occur simultaneously with those of the SST and the $\delta^{18}O$ of *G. ruber*. For example, the rapid increases of the Mn/Ca ratios during Termination I and Termination II appear to occur before the rapid changes of the SSTs and the $\delta^{18}O$.

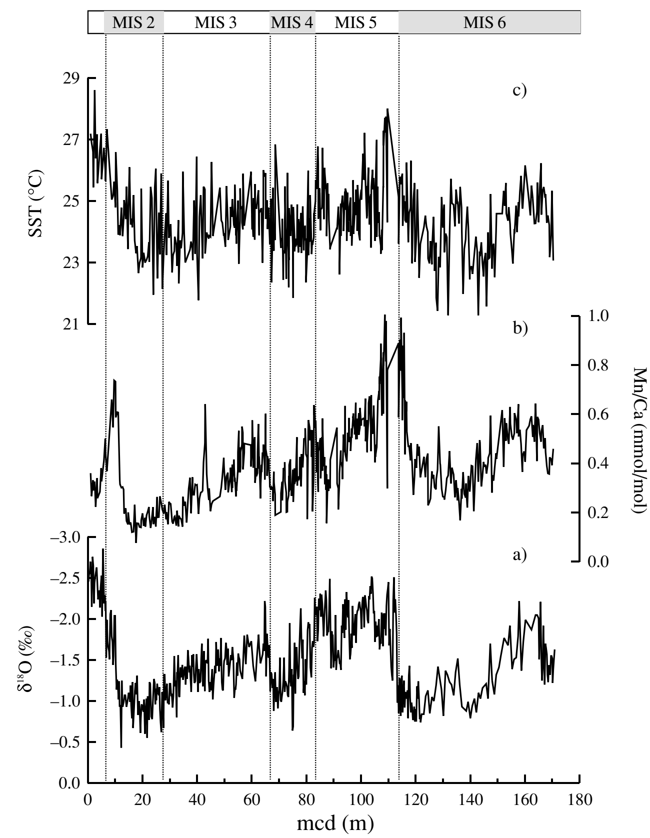

Fig. 2. Variations of the Mn/Ca ratios of G. sacculifer at ODP Site 1144 and other paleoclimate records of ODP Site 1144. a) oxygen isotopes of G. ruber; b) SSTs derived from Mg/Ca ratios of G. sacculifer; c) Mn/Ca ratios of G. sacculifer; The vertical lines indicate the boundaries of MIS stages.

DISCUSSIONS

Response to paleoclimate change

As shown in Fig. 2, the variation pattern of the Mn/Ca ratios of *G. sacculifer* is similar to those of the SSTs and the $\delta^{18}O$ of *G. ruber*, which are broadly used to indi-

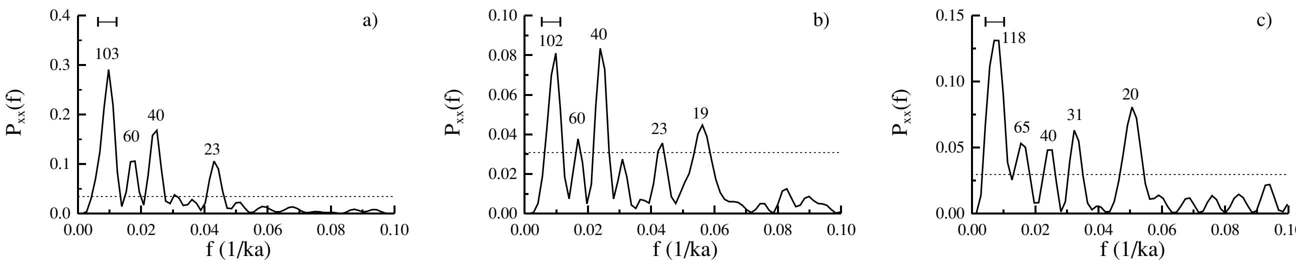

Fig. 3. Harmonic analysis (Siegel's test) of the paleoclimate records at ODP Site 1144 using SPECTRUM (Schulz and Stattegger, 1997). a) oxygen isotopes of G. ruber; b) SSTs derived from Mg/Ca ratios of G. sacculifer; c) Mn/Ca ratios of G. sacculifer; Setting: OFAC = 2, HIFAC = 1, α = 0.05, λ = 0.4; horizontal bars mark the 6-dB bandwidths; dashed lines indicate the 95% confidence intervals. Numbers represent the respective periodicities of the peaks.

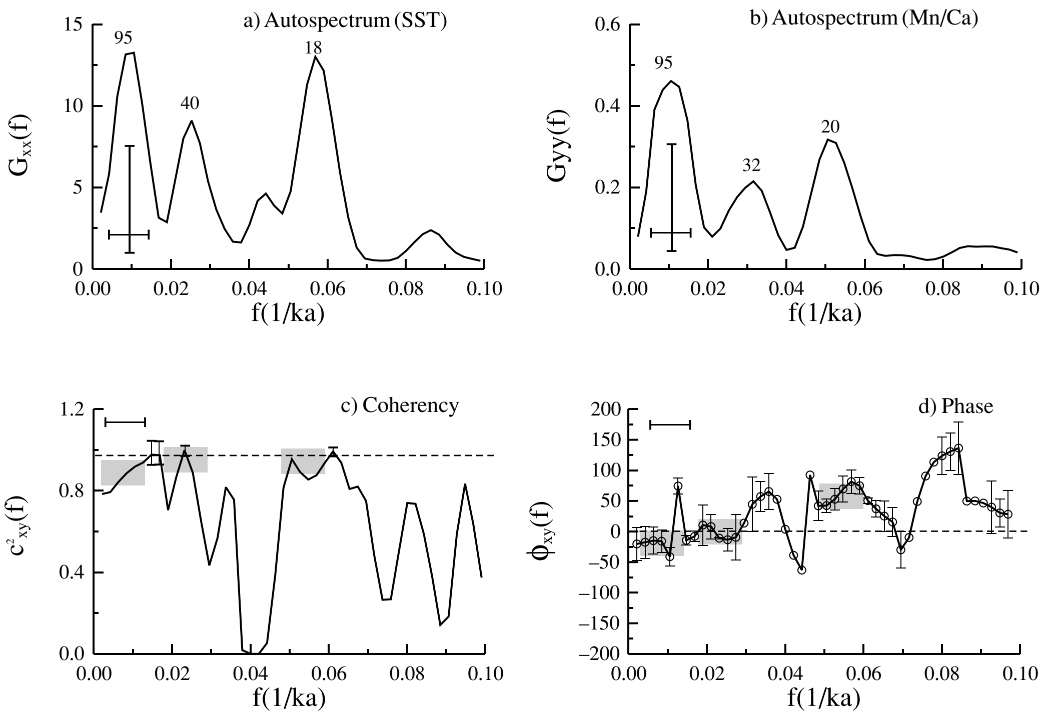

Fig. 4. Cross spectral analysis between SSTs and Mn/Ca ratios of G. sacculifer at ODP Site 1144 using SPECTRUM (Schulz and Stattegger, 1997). Setting: OFAC = 4, HIFAC = 1, N_{seg} = 2, Welch window; a) Autospectrum for SST: The horizontal and vertical error bars mark 6-dB bandwidth and 90% confidence interval, respectively; b) as a) but for Mn/Ca ratios; c) Coherency between the two time series: The horizontal error bar marks 6-dB bandwidth, the dashed line marks indicates false alarm level (α = 0.1), and the shaded bars mark the range of the orbital periodicities within 6-dB bandwidth; d) Phase angles between SST and Mn/Ca ratios: the shaded bars mark the range of the orbital periodicities within 6-dB bandwidth.

cate paleoclimate changes. Thus, the variation of the Mn/Ca ratios may probably response to some climatic/environmental processes related to paleoclimate changes. Power spectra of paleoclimate records can show their variation periodicities of their main variations, and are generally used to seek for hints of their driven forcing in paleoceanography studies. Here, we show the power spectra calculated using the software of SPECTRUM (Schulz and Stattegger, 1997) of the SSTs, $\delta^{18}O$ and Mn/Ca ratios of planktonic foraminifers from the sediments at ODP Site 1144 in Fig. 3. Robust periodicities centering at 103 kyr, 60 kyr, 40 kyr and 23 kyr are clearly shown in the power spectrum of the $\delta^{18}O$ of *G. ruber* (Fig. 3a). Except for the 60 kyr periodicity, which may be the result of periodicity interaction, the other three periodicities may correspond to the ~100 kyr eccentricity cycle, ~41 kyr obliquity cy-

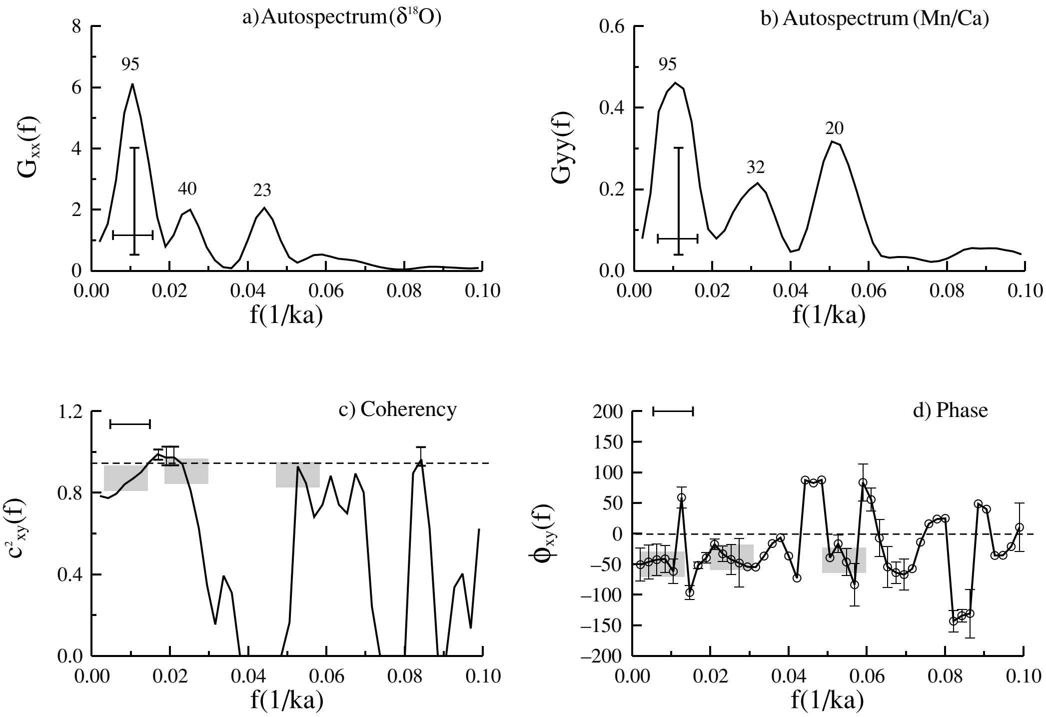

Fig. 5. Cross spectral analysis between $\delta^{18}O$ of G. ruber and Mn/Ca ratios of G. sacculifer at ODP Site 1144 using SPECTRUM (Schulz and Stattegger, 1997). The setting and the marks are the same as those in Fig. 4. The variation of the $\delta^{18}O$ of G. ruber has been inverted before calculation.

cle and 21~23 kyr precession cycle within the 6-dB bandwidth, which are the characteristic periodicities for the Earth's orbital variations. The periodicities occurring in the spectrum of the SSTs are nearly the same as those in the spectrum of the δ^{18}O of *G. ruber* except that the two precession cycles are presented separately centering at 23 kyr and 19 kyr, respectively (Fig. 3b). The robust periodicities in the spectrum of the Mn/Ca ratios of *G. sacculifer* center at 118 kyr, 65 kyr, 40 kyr, 31 kyr and 20 kyr (Fig. 3c). The 118 kyr periodicity may correspond to the ~100 kyr eccentricity cycle, and the 65 kyr periodicity appears to correspond to the ~60 kyr periodicity in the other two spectra within the 6-dB bandwidths. The periodicities centering at 40 kyr and 20 kyr may represent the obliquity and precession cycles, respectively. Therefore the characteristic orbital periodicities are all significantly presented in the spectrum of the Mn/Ca ratios of *G. sacculifer*, suggesting that the variation of the Mn/Ca ratios mainly responses to paleoclimate changes driven by orbital forcing. However, very little is known about the 31 kyr periodicity, which is not presented in the spectra of the SSTs and the δ^{18}O of *G. ruber*, implying that some other unknown factors also influence the variation of the Mn/Ca ratios of *G. sacculifer*.

Even though the variation patterns are similar, the variation of the Mn/Ca ratios is not always in pace with the other two paleoclimate records as shown in Fig. 2. The leads and lags between the variations of the Mn/Ca ratios and the other records may help to find more details of the response of the Mn/Ca ratios to paleoclimate changes because the physical processes represented by the SSTs and the δ^{18}O of *G. ruber* are different. The SST record mainly indicates changes of the sea surface temperature, whereas the variation of the δ^{18}O of *G. ruber* is controlled both by changes of ice volume at continents and sea surface temperature. We now perform cross spectral analysis between the record of the Mn/Ca ratios and the other two paleoclimate records to compare their variation paces.

Figure 4 shows the cross spectra between the SSTs and the Mn/Ca ratios calculated using the SPECTRUM software (Schulz and Stattegger, 1997). The eccentricity cycle, obliquity cycle and precession cycle are clearly presented (Figs. 4a and 4b). The coherencies between these two records at these three periodicities are all close or higher than the 90% false alarm level indicated by the horizontal dashed line in Fig. 4c, suggesting that the correlation between the variations of the SSTs and the Mn/Ca ratios is significant. The phase angles around the eccentricity cycle range from –41° to –15° with an average of –25 ± 18° (Fig. 4d). Similarly, the phase angles around the obliquity cycle vary from –14° to 8°, and average at

$-11 \pm 3°$. This suggests that the SST variations are nearly in pace with or slightly lag behind those of the Mn/Ca ratios at the eccentricity and obliquity cycles. The phase angles at the precession cycle vary from 42° to 81° with an average of $60 \pm 22°$, indicating that the SST variation lead ahead of that of the Mn/Ca ratios at the precession cycle.

The cross spectra between the $\delta^{18}O$ of *G. ruber* and the Mn/Ca ratios are shown in Fig. 5. Like those between the SSTs and the Mn/Ca ratios, the three characteristic orbital cycles are clearly exhibited, and the coherencies between the two records at these periodicities are close to or higher than the 90% false alarm level (Fig. 5), suggesting significant correlation. However, the phase angles are different. The averages of the phase angles at the eccentricity cycle, the obliquity cycle and the precession cycle are $-50 \pm 21°$, $-25 \pm 13°$ and $-32 \pm 67°$, respectively (Fig. 5d), indicating that the variations of the $\delta^{18}O$ of *G. ruber* generally lag behind those of the Mn/Ca ratios at the orbital periodicities.

The above spectral analysis results suggests that the variation of the Mn/Ca in *G. sacculifer* actively responses to paleoclimate changes driven by orbital forcing. The changes of the Mn/Ca ratios generally lead those of the $\delta^{18}O$ of *G. ruber* at orbital periodicities, and they appear to be in pace with the SSTs at the eccentricity and obliquity periodicities, but significantly lag behind of the SSTs at the precession period. Therefore, the Mn/Ca ratios in *G. sacculifer* may potentially an indicator for paleoclimate changes.

The meaning of the Mn/Ca ratios of G. sacculifer

As mentioned above, the variation of the Mn/Ca ratios of *G. sacculifer* at ODP Site 1144 is closely related to paleoclimate changes. However, what kind of climatic or environmental change it indicates is still not clear. Considering that the behaviors of Mn in sediments are very sensitive to change of redox conditions, and the two phases of Mn-coatings in foraminifer tests are closely associated with redox conditions, the variation of the Mn/Ca ratios of *G. sacculifer* is supposed to relate to redox condition change in sediments too.

Figure 6 shows the down-core variation of the Mn/Ca ratios of *G. sacculifer* and some of the geochemical records that are sensitive to changes of redox condition. The authigenic Mn concentration, which may be the estimate for Mn oxide content, is one of the best indices to evaluate redox conditions in sediments (Calvert and Pedersen, 1993; Mangini *et al.*, 2001). The chemical composition of both bulk and detrital components of the sediments from ODP Site 1144 have been reported (Wei *et al.*, 2004, 2003). Supposing that Ti is mostly contributed from detrital components (Wei *et al.*, 2003), the concentration of authigenic Mn in the sediments can be calculated by following equation:

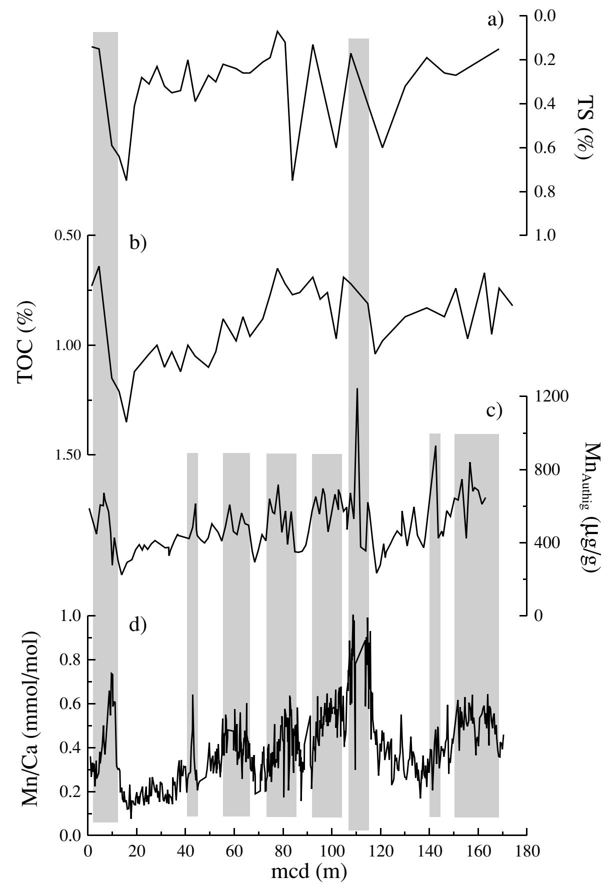

Fig. 6. Variations of the Mn/Ca ratios of G. sacculifer, authigenic Mn concentrations and contents of TOC and TS at ODP Site 1144. a) TS contents; b) TOC contents; c) authigenic Mn concentrations; d) Mn/Ca ratios of G. sacculifer. Note that the axes for TS and TOC contents are in descending order. Vertical shaded bars mark the correlations between different records.

$$Mn_{authigenic} = Mn_{bulk} - Ti_{bulk} \times (Mn/Ti)_{detrital}.$$

In addition to authigenic Mn concentration, the content of total sulfur (TS) can also indicate redox condition in sediments because sulfur tends to deposit in sediments as sulfide in reductive environment and dissolve in interstitial water as sulfate in oxic environment (Froelich *et al.*, 1979). Organic matters are the most important reductant in sediments, thus the variation of total organic carbon (TOC) contents are also shown in Fig. 6. The TS and TOC contents of the sediments at ODP Site 1144 refer from the initial reports of Leg 184 (Shipboard Scientific Party, 2000). Even though the time-resolution for the TS and TOC records is fair low, their variations can still be correlated to those of the authigenic Mn concentration.

Generally, decreasing of TS contents correspond to decreasing of TOC contents and increasing of authigenic Mn concentrations, and *vice versa* (Fig. 6). In particular, during the main climate boundaries, such as Termination I and II, these geochemical records appear to vary simultaneously (Fig. 6). The consistency among these geochemical records suggests that they can reliably indicate redox condition changes in the sediment at ODP Site 1144.

As show in Fig. 6, the authigenic Mn concentrations vary from ~200 μg/g to ~1200 μg/g, about 2~4 times of the Mn concentrations in the detrital components (Wei *et al.*, 2003), indicating that Mn oxides have not been consumed in the sediments from which the foraminifer tests were picked up. Thus, the extreme reductive condition enabling Ca–Mg–Mn carbonates to be formed seems not occur in these sediments (Calvert and Pedersen, 1993), and the Mn coatings in these foraminifer tests are mainly associated with Mn oxides. This can also be supported by the similar variation patterns of the Mn/Ca ratios of *G. sacculifer* and the authigenic Mn concentrations (Fig. 6). Even though quantitative evaluation of the similarity between these two records, such as cross spectral analysis, is difficult to be handled for the large gap of time resolution between these two records, which are about 0.33 kyr and 1.5 kyr for the Mn/Ca ratios of *G. sacculifer* and the authigenic Mn concentrations, respectively, the correlation between the variations of these two records is still obvious. As highlighted by the shaded bars in Fig. 6, most of the oscillations of the Mn/Ca ratios are accompanied by similar variations of the authigenic Mn concentrations, and higher Mn/Ca ratios generally correlate to higher authigenic Mn concentrations. Therefore, the variation of the Mn/Ca ratios of *G. sacculifer* at ODP Site 1144 is closely associated with that of the authigenic Mn concentrations, and indicates changes of redox conditions in sediments.

It is worthy noting that the upward decreasing of the Mn/Ca ratios of *G. sacculifer* at the top 10 mcd is different from those of the other paleoclimate records (Fig. 2). As shown in Fig. 6 the TS and TOC contents are low, and the authigenic Mn concentrations are high in this section, suggesting an oxic environment. Thus, high Mn/Ca ratios of *G. sacculifer* are expected if the Mn/Ca ratios mainly indicate the redox conditions in sediments. This, however, does not agree with the observed variation of the Mn/Ca ratios at the top 10 mcd. Though the exact reasons for this is hard to be told currently, the Mn/Ca ratios of *G. sacculifer* from core-top sediments from the SCS may provide hints. The Mn/Ca ratios of core-top *G. sacculifer* are fairy low as shown in Fig. 1, which range from 0.02 mmol/mol to 0.49 mmol/mol with an average of 0.17 ± 0.16 (1σ) mmol/mol. If the two samples with high Mn/Ca ratios from the southern SCS are excluded, the average is even much lower, 0.11 ± 0.08 (1σ) mmol/mol. In contrast, the grand mean of the Mn/Ca ratios of *G. sacculifer* at ODP Site 1144 is 0.41 ± 0.16 (1σ) mmol/mol, significantly higher than that of the core-top samples. This implies that the growing of the Mn coatings on foraminifer tests does not occur at the surface of sediments, but inside sediments right after burial. Considering that most Mn oxides are generated at the maximum depth for O_2 to penetrate to, which is generally located in the top several to tens of centimeters of the sediment column, rather than at the surface of sediments (Froelich *et al.*, 1979; Mangini *et al.*, 1990, 2001). When Mn(II) is oxidized at the oxic-suboxic interface, it is firstly transformed into Mn(III) and deposited as MnOOH in sediments, and MnOOH is further oxidized into Mn(IV) as MnO_2 during burial (Anschutz *et al.*, 2005; Hem and Lind, 1983). Considering that MnOOH is not as stable as MnO_2 (Hem and Lind, 1983), MnOOH may gradually be decomposed, and MnO_2 may gradually be generated in sediment column. If only MnO_2 rather than MnOOH is overgrown on foraminifer tests, downward increasing of Mn contents in foraminifer tests may occur in the top most section of sediment column. This appears to reasonably interpret the upward decreasing of the Mn/Ca ratios of *G. sacculifer* at the top 10 mcd at ODP Site 1144. However, the time for MnOOH to age and transform into MnO_2 is not very long, and this generally occurs in the top several to tens of centimeters in sediment column (Anschutz *et al.*, 2005). In contrast, the depth of the downward increasing of Mn/Ca ratios at ODP Site 1144 is up to 10 m, with time span of about 10 kyr. Therefore, this is still not a convinced interpretation, and further studies, such as detailed oxidation states of authigenic Mn in foraminifer tests and sediments of the top section at ODP Site 1144, are needed. Despite of the complicated variations at the top 10 mcd, the response of the Mn/Ca ratios of *G. sacculifer* to paleoclimate changes is significant, and the correlation between the Mn/Ca ratios and redox conditions in sediments is significant too. Thus, the record of the Mn/Ca ratios of *G. sacculifer* is an informative paleoclimate indicator, which might proxy redox condition in sediments.

Summary

We report high-resolution Mn/Ca ratios of *G. sacculifer* from sediments at ODP Site 1144 in the northern SCS in this paper to show that the Mn/Ca ratios of planktonic foraminifer tests may be a possible paleoclimate indicator:

1) The variation pattern of the Mn/Ca ratios is similar to those of the other paleoclimate records, such as the $\delta^{18}O$ of *G. ruber* and the SSTs derived from Mg/Ca ratios of *G. sacculifer*. The results of spectral analysis indicate

that similar to the other paleoclimate records, the power spectrum of the Mn/Ca ratios show robust Milankovitch periodicities, such as ~100 kyr eccentricity cycle, ~41 kyr obliquity cycle and 21~23 kyr precession cycle. This indicates that the variation of the Mn/Ca ratios mainly responses to paleoclimate changes driven by orbital forcing. Further comparisons by cross spectral analysis indicate that the variation of Mn/Ca ratios of *G. sacculifer* leads that of the δ^{18}O of *G. ruber* at these orbital periodicities, and slightly leads or is roughly in pace with that of the SSTs at eccentricity and obliquity cycles, but lags behind that of the SSTs at precession cycle. Therefore, the driven forcing for the variation of the Mn/Ca ratios seems mainly to associate with those for the SSTs.

2) The variation of the Mn/Ca ratios of *G. sacculifer* appears to correlate to those of the proxies for redox condition in sediments, such as authigenic Mn concentrations, TS and TOC contents. Generally, higher Mn/Ca ratios correspond to higher authigenic Mn concentrations and lower TS and TOC contents. This indicates that the Mn coatings in the *G. sacculifer* at ODP Site 1144 mainly associate with Mn oxides, and the variation of the Mn/Ca ratios indicates changes of redox condition in the sediments.

3) At the top 10 mcd, the Mn/Ca ratios show an upward decreasing trend, which does not agree with the other paleoclimate records. The low Mn/Ca ratios at this section seem conflict with the oxic environment, but agree with the general low Mn/Ca ratios of *G. sacculifer* from core-top samples in the SCS. The within sediment column location for Mn oxides to be generated and changes of oxidation states for authigenic Mn after sediment burial, such as transformation from Mn(III) oxyhydroxides to Mn(IV) oxides, account for such variation of the Mn/Ca ratios at the top 10 mcd. Details, however, are not clear yet, and further studies are needed.

Acknowledgments—The sediment samples of ODP Site 1144 were provided by Ocean Drilling Project (ODP). The authors thank the critical comments from the two anonymous reviewers, which help to improve the manuscript. Thanks also go to Dr. Weidong Sun of the Guangzhou Institute of Geochemistry, CAS for his help in polishing the English of this manuscript. This work was supported by the Chinese Academy of Sciences (Grant KZCX2-YW-318), the Chinese Ministry of Science and Technology Special Scheme (Grant 2007CB815905), and the National Natural Science Foundation of China (Grant 40673075). This is contribution No. IS-1031 from GIGCAS.

REFERENCE

Anschutz, P., Dedieu, K., Desmazes, F. and Chaillou, G. (2005) Speciation, oxidation state, and reactivity of particulate manganese in marine sediments. *Chem. Geol.* **218**, 265–279.

Barker, S., Greaves, M. and Elderfield, H. (2003) A study of cleaning procedures used for foraminiferal Mg/Ca paleothermometry. *Geochem. Geophys. Geosyst.* **4**, 8407, doi:10.1029/2003GC000559.

Boyle, E. A. (1981) Cadmium, zinc, copper and barium in foraminifera tests. *Earth Planet. Sci. Lett.* **53**, 11–36.

Boyle, E. A. (1983) Manganese carbonate overgrowths on foraminifera tests. *Geochim. Cosmochim. Acta* **47**, 1815–1819.

Büehring, C., Sarnthein, M. and Erlenkeuser, H. (2004) Toward a high-resolution stable isotope stratigraphy of the last 1.1 million years, ODP Site 1144, South China Sea. *Proc. Ocean Drill Prog., Sci. Results*.

Calvert, S. E. and Pedersen, T. F. (1993) Geochemistry of recent oxic and anoxic marine-sediments: Implications for the geological record. *Mar. Geol.* **113**, 67–88.

Elderfield, H. and Ganssen, G. (2000) Past temperature and δ^{18}O of surface ocean waters inferred from foraminiferal Mg/Ca ratios. *Nature* **405**, 442–445.

Froelich, P. N., Klinkhammer, G. P., Bender, M. L., Luedtke, N. A., Heath, G. R., Cullen, D., Dauphin, P., Hammond, D., Hartman, B. and Maynard, V. (1979) Early oxidation of organic matter in pelagic sediments of the eastern equatorial Atlantic: Suboxic diagenesis. *Geochim. Cosmochim. Acta* **43**, 1075–1090.

Hastings, D. W., Russell, A. D. and Emerson, S. R. (1998) Foraminiferal magnesium in *Globeriginoides sacculifer* as a paleotemperature proxy. *Paleoceanography* **13**, 161–169.

Hem, J. D. and Lind, C. J. (1983) Nonequilibrium models for predicting forms of precipitated manganese oxides. *Geochim. Cosmochim. Acta* **47**, 2037–2046.

Landing, W. M. and Bruland, K. W. (1987) The contrasting biogeochemistry of iron and manganese in the Pacific Ocean. *Geochim. Cosmochim. Acta* **51**, 29–43.

Lea, D. W., Mashiotta, T. A. and Spero, H. J. (1999) Controls on magnesium and strontium uptake in planktonic foraminifera determined by live culturing. *Geochim. Cosmochim. Acta* **63**, 2369–2379.

Lea, D. W., Martin, P. A., Pak, D. K. and Spero, H. J. (2002) Reconstructing a 350 ky history of sea level using planktonic Mg/Ca and oxygen isotope records from a Cocos Ridge core. *Quarter. Sci. Rev.* **21**, 283–293.

Lea, D. W., Pak, D. K., Belanger, C. L., Spero, H. J., Hall, M. A., Shackleton, N. J. (2006) Paleoclimate history of Galapagos surface waters over the last 135,000 yr. *Quarter. Sci. Rev.* **25**, 1152–1167.

Mangini, A., Eisenhauer, A. and Walter, P. (1990) Response of Manganese in the ocean to the climatic cycles in the Quaternary. *Paleoceanography* **5**, 811–821.

Mangini, A., Jung, M. and Laukenmann, S. (2001) What do we learn from peaks of uranium and of manganese in deep sea sediments? *Mar. Geol.* **177**, 63–78.

Mashiotta, T. A., Lea, D. W. and Spero, H. J. (1999) Glacial-interglacial changes in Subantarctic sea surface temperature and δ^{18}O-water using foraminiferal Mg. *Earth Planet. Sci. Lett.* **170**, 417–432.

Nürnberg, D. and Groeneveld, J. (2006) Pleistocene variability of the Subtropical Convergence at East Tasman Plateau: Evidence from planktonic foraminiferal Mg/Ca (ODP Site 1172A). *Geochem. Geophys. Geosyst.* **7**, Q04P11, doi:10.1029/2005GC000984.

Nürnberg, D., Bijma, J. and Hemleben, C. (1996) Assessing the reliability of magnesium in foraminiferal calcite as a proxy for water mass temperatures. *Geochim. Cosmochim. Acta* **60**, 803–814.

Pena, L. D., Calvo, E., Cacho, I., Eggins, S. and Pelejero, C. (2005) Identification and removal of Mn–Mg-rich contaminant phases on foraminiferal tests: Implications for Mg/Ca past temperature reconstructions. *Geochem. Geophys. Geosyst*. **6**, Q09P02, doi:10.1029/2005GC000930.

Rosenthal, Y., Lohmann, G. P., Lohmann, K. C. and Sherrell, R. M. (2000) Incorporation and preservation of Mg in *Globigerinoides sacculifer*: Implications for reconstructing the temperature and $^{18}O/^{16}O$ of seawater. *Paleoceanography* **15**, 135–145.

Schulz, M. and Stattegger, K. (1997) SPECTRUM: Spectral analysis of unevenly spaced paleoclimatic time series. *Comp. & Geosci*. **23**, 929–945.

Shipboard Scientific Party (2000) Site 1144. *Proc. ODP, Init Repts., 184* [CD-ROM] (Wang, P., Prell, W. L. and Blum, P., eds.), 1–97, available from, Ocean Drilling Program, Texas A&M University, College Station TX 77845-9547, U.S.A.

Wei, G. J., Liu, Y., Li, X. H., Shao, L. and Liang, X. R. (2003) Climatic impact on Al, K, Sc and Ti in marine sediments: Evidence from ODP Site 1144, South China Sea. *Geochem. J*. **37**, 593–602.

Wei, G. J., Liu, Y., Li, X. H., Shao, L. and Fang, D. Y. (2004) Major and trace element variations of the sediments at ODP Site 1144, South China Sea, during the last 230 ka and their paleoclimate implications. *Palaeogeogr. Palaeoclimatol. Palaeoecol*. **212**, 331–342.

Wei, G. J., Deng, W. F., Li, X. H. and Liu, Y. (2007) High-resolution sea surface temperature records derived from foraminiferal Mg/Ca ratios during the last 260 ka in the northern South China Sea. *Palaeogeogr. Palaeoclimatol. Palaeoecol*. **250**, 126–138.

Weldeab, S., Schneider, R. R. and Kolling, M. (2006) Comparison of foraminiferal cleaning procedures for Mg/Ca paleothermometry on core material deposited under varying terrigenous-input and bottom water conditions. *Geochem. Geophys. Geosyst*. **7**, Q04P12, doi:10.1029/2005GC000990.

Yu, J. M., Elderfield, H., Greaves, M. and Day, J. (2007) Preferential dissolution of benthic foraminiferal calcite during laboratory reductive cleaning. *Geochem. Geophys. Geosyst*., **8**, Q06016, doi:10.1029/2006GC001571.